these values is below 30 nsec for four experimental conditions (See Tables). The initial kinetic energy of Zn^+ ion is found to be 22-44 kJ/mol at laser power of about 5×10^7 W/cm^2. These values are equivalent to the velocities of 8×10^5-1.1×10^6 cm/s and the surface temperature of 2670-5100 K. Time-of-flight measurement of Zn^+ ion indicates that its energy is very low. Similar results for the initial kinetic energy also were obtained by the pulsed copper ablation.[18]

Conclusions

The flight time measurement of an ion as a function of the time delay between the ablation laser and extraction pulses has been demonstrated to be a useful method of obtaining the initial kinetic energy of an ion. The time-of-flight dependence of an ion on time delay has been formulated and fitted into experimental data to obtain the initial kinetic energy of the ablated ion. At 532 nm and about 5×10^7 W/cm^2 power, the initial kinetic energy of ablated ions have been found to be 22-44 kJ/mol.

Acknowledgment. This work was supported by the Ministry of Science and Technology.

References

1. Ledingham, K. W. D.; Singhal, R. P. In *Applied Laser Spectroscopy: Techniques, Instrumentation, and applications*; VCH Publisher: New York, 1992; Chap. 9.
2. Bauerle, D. *Laser Processing and Chemistry, 2nd Ed.*; Springer-verlag: Berlin, 1996.
3. Alimpiev, S. S.; Belov, M. E.; Nikiforov, S. M. *Anal. Chem.* **1993**, *65*, 3194.
4. Wang, L.; Borthwick, I. S.; Jennings, R.; McCombes, P. T.; Ledingham, K. W. D.; Singhal, R. P.; McLean, C. J. *Appl. Phys. B* **1991**, *53*, 34.
5. Consalvo, A. M.; Stranges, D.; Giardini-Guidoni, A.; Teghil, R. *int. J. Mass A Spectrom. Ion Proc.* **1990**, *95*, 359.
6. Miller, J. C. *Laser Ablation: Principles and Applications*; Springer-verlag: Berlin, 1994.
7. Demtrder, W.; Jantz, W. *Plasma Phys.* **1970**, *12*, 691.
8. Srinivasan, R.; Braren, B. *Chem. Rev.* **1989**, *89*, 1303.
9. Zweig, A. D. *J. Appl. Phys.* **1991**, *70*, 1684.
10. Pettit, G. H.; Sauerbrey, R. *Appl. Phys. A* **1993**, *56*, 2909.
11. Kovalev, I. D.; Maksimov, G. A.; Larin, N. V. *Int. J. Mass. Spectrom. Ion Phys.* **1978**, *27*, 101.
12. Zheng, J. P.; Huang. Z. Q.; Shaw, D. T; Kwok, H. S. *Appl. Phys. Lett.* **1985**, *54*, 280.
13. Kool, J. C. S.; Brongersma, S. H.; van de Riet, E.; Dieleman, J. *Appl. Phys. B* **1991**, *53*, 125.
14. Ulmer, G.; Hasselberger, B.; Busmann, H.-G. Campbell, E. E. B. *Appl. Sur. Sci.* **1990**, *46*, 272.
15. Namiki, A.; Watabe, K.; Fukano, H.; Nishigaki, S.; Noda, T. *J. Appl. Phys.* **1983**, *54*, 3443.
16. Im, H.-S.; Yoon, H.-S.; Kim, K. S. to be published.
17. Wiley, W. C.; McLaren, I. H. *Rev. Sci. Instrum.* **1955**, *26*, 1150.
18. von Gutfeld, R. J.; Dreyfus, R. W. *Appl. Phys. Lett.* **1986**, *54*, 1212.

Synthesis and Properties of Terdentates with Extra Pyridine Ring and Their Ru(II) Complexes

Yurngdong Jahng*, Seung Wook Moon, and Randolph P. Thummel†

College of Pharmacy, Yeungnam University, Kyongsan 712-749, Korea
†Department of Chemistry, University of Houston, Houston, TX 77204-5641, USA
Received October 23, 1996

The synthesis and electronic as well as redox properties of four Ru(II) complexes based on the ligand 4'-(4-pyridyl)-3,3';5',3"-bis-dimethylene-2,2';6',2"-terpyridine are reported. Each new complex is of the type $[Ru(L)_2]^{n+}$ and $[Ru(tpy)(L)]^{n+}$, where L is the terdentate ligand with extra pyridine ring at 4'-position or is a N-methylated ligand and n=2, 3, or 4. Cyclic voltammetry indicates that the first electron added to the complex enters the viologen-type acceptor in N-methylated ligand.

Introduction

Importance of polypyridines, especially 2,2'-bipyridine (bpy) and 2,2';6',2"-terpyridine(tpy), stems from their abilities to form complexes with various transition metals. Ruthenium(II) complexes of these polypyridines, show somewhat unique spectroscopic,[1] electrochemical,[2] photophysical and photochemical[3] and biochemical properties[4] compared to other transition metals. Studies on the photophysical and photochemical properties of the ruthenium complexes have been directed toward electron transfer quenching process of the excited state to lead to energy storing redox products. Among the oxidative quenching agents, pyridinium ions, including viologen have most likely been employed. For the biochemical properties, some of ruthenium complexes exhibit intercalative binding to DNA and

show promising site specific probes for polynucleotides.

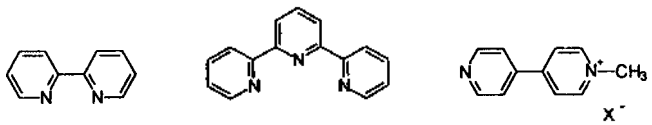

2,2'-bipyridine (bpy) 2,2';6',2"-terpyridine (tpy) viologen

Recent studies are focused on the rational design and synthesis of ligands as well as their complexes to pursue such desired properties. Most of systems, so far introduced, include 2,2'-bipyridine unit to form $Ru(bpy)_2(L)^{2+}$ complex while a system with 2,2';6',2"-terpyridine is relatively rare.[5] We herein describe design and synthesis of new terdentates (**1**) which have electron donating metal center and viologen-type electron acceptor in the same molecule upon complexation of the N-methylated ligand.

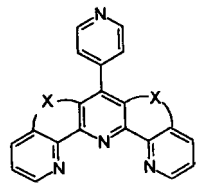

1a X = H, H
b X = $-(CH_2)_2-$

Experimental

Melting points were determined on a Fisher-Jones melting point apparatus and are not corrected. Infrared spectra were recorded on a Perkin Elmer 1330 spectrophotometer. Nuclear magnetic resonance spectra were obtained on a Varian Associates FT-80 spectrometer or a Nicolet NT-300 WB spectrometer. Chemical shifts are given in parts per million downfield from Me_4Si. Ultraviolet spectra were obtained on a Perkin Elmer 330 spectrophotometer. Mass spectra were obtained by direct sample introduction into a Hewlett-Packard 5933A GC-Mass spectrometer or by introduction as a 0.1 M NH_4OAc solution into a Biospec LC-MS spectrometer with a thermospray ionization interface. Cyclic voltammetric measurement were carried out on a IBM Instrument Model EC-225 Voltammetric Analyzer utilizing a three electrode system. The working electrode consisted of a 20 gauge Pt wire connected to a 24 gauge copper wire and embedded flush at the tip of 5 mm (o.d.) pyrex glass tube. A saturated KCl calomel solution by a cracked glass bridge filled with 0.1 M TBAP (tetra-*n*-butylammonium perchlorate) in acetonitrile. The counter electrode consisted of a 20 gauge Pt wire inserted directly into the solution. Deaeration of all solutions was performed by passing high purity nitrogen through the solution for five minutes and maintaining a nitrogen atmosphere over the solution while making measurements. A Hewlett-Packard X-Y Recorder was used to record the cyclic voltammograms. Halfwave potentials ($E_{1/2}$) were measured as the average of the anodic and cathodic peak potentials. Scan rates varied from 50-200 mV/sec. Electrochemical reversibility was judged on the basis of the following criteria:[6] (a) The separation of the anodic and cathodic peak potentials (ΔE) equals 60/n mV where n is the number of electrons involved in the redox process. (b) The ratio of the anodic and cathodic peak currents ($i_{p,a}/i_{p,c}$) is unity regardless of the scan rates. All solvents were freshly distilled reagent grade. Acetonitrile was distilled from CaH_2 under argon atmosphere for cyclic voltammetry. $Ru(tpy)Cl_3$,[7] and 2-(1-morpholinovinyl)pyridine (**2a**)[8] and 8-morpholino-5,6-dihydroquinoline (**2b**)[9] were prepared by previously described procedure.

4'-(4-pyridyl)-2,2';6',2"-terpyridine (1a). A solution of 5.00 g (26.0 mmol) of **2a** and 1.31 g (13.0 mmol) of 4-pyridinecarboxaldehyde in 20 mL of dioxane was refluxed for 10 h. The mixture was cooled, made acidic with 5 N HCl, and the organic layer was separated. The aq. layer was made basic with 50% NaOH and extracted with CH_2Cl_2 (50 mL×3). The organic layer was dried over $MgSO_4$ and the solvent was evaporated. The crude material was not identified but rather treated with 3 g of NH_4OAc in 30 mL of acetic acid at 150 °C for 3 h. After cooling, the solution was made basic with 50% NaOH and extracted with CH_2Cl_2 (50 mL×3). The organic layer was dried over $MgSO_4$. Evaporation of the solvent gave a residue which was chromatographed on alumina eluting with CH_2Cl_2. The early fractions gave 0.82 g (20%) of a desired product as a pale yellow solid: mp 224-225 °C. ^1H NMR ($CDCl_3$, 80 MHz) δ 8.79-8.61 (m, 8H), 7.88 (dd, 2H, *J*=7.7, 1.7 Hz, H4' and H 4"), 7.78 (d, 2H, *J*=4.8 Hz, H3'"), 7.35 (dd, 2H, *J*=7.7, 4.8 Hz, H5' and H5"); ^{13}C NMR ($CDCl_3$, 20 MHz) δ 156.4, 155.7, 150.5, 149.2, 147.4, 145.9, 136.9, 124.0, 121.6, 121.3, 118.6; IR (KBr) ν 3060, 2960, 1600, 1550, 1440, 1410, 1380, 1220, 1100, 900 cm^{-1}; MS, m/e (rel. intensity) 300 (100, M), 299 (90, M-1), 233 (37), 91 (21), 65 (19). Anal. Calcd for $C_{20}H_{14}N_4$-H_2O: C, 73.17; H, 4.88; N, 17.07. Found: C, 72.95; H, 4.85; N, 17.09.

4'-(4-Pyridyl)-3,3';5',3"-bis(dimethylene)-2,2';6',2"-terpyridine (1b). A solution of 2.16 g (10.0 mmol) of 8-morpholino-5,6-dihydroquinoline and 0.60 g (5.60 mmol) of 4-pyridinecarboxaldehyde in 20 mL of dioxane was refluxed for 10 h. The mixture was cooled, made acidic with 5 N HCl, and the organic layer was separated. The aq. layer was made basic with 50% NaOH and extracted with CH_2Cl_2 (50 mL×3). The organic layers were dried over $MgSO_4$ and the solvent was evaporated. The crude material was not identified but rather treated with 3 g of NH_4OAc in 30 mL of acetic acid at 150 °C for 3 h. After cooling, the solution was made basic with 50% NaOH and extracted with CH_2Cl_2 (50 mL×3). The organic layer was dried over $MgSO_4$. Evaporation of the solvent gave a residue which was chromatographed on alumina eluting with CH_2Cl_2. The early fractions gave 1.08 g (56%) of a desired product as a pale yellow solid: mp > 300 °C. ^1H NMR ($CDCl_3$, 80 MHz) 8.79 (d, 2H, *J*=4.8 Hz, H2'"), 8.75 (dd, 2H, *J*=4.8, 0.6 Hz, H6), 7.58 (dd, 2H, *J*=7.7, 0.6 Hz, H4' and H4"), 7.29 (dd, 2H, *J*=7.7, 4.8 Hz, H5' and H5"), 7.19 (d, 2H, *J*=4.8 Hz, H3'"), 2.91 (t, 2H, *J*=6.7 Hz), 2.67 (t, 2H, *J*=6.7 Hz); ^{13}C NMR ($CDCl_3$, 20 MHz) δ 151.1, 150.1, 149.7, 148.2, 144.6, 144.1, 134.7, 132.5, 130.6, 123.0, 122.8, 26.5, 24.8; IR (KBr) ν 3060, 2962, 1600, 1570, 1550, 1442, 1410, 1390, 1220, 1100, 900 cm^{-1}; MS, m/e (rel. intensity) 362 (100, M), 361 (92, M-1), 149 (40), 91 (19), 65 (19). Anal. Calcd for $C_{24}H_{18}N_4$-$0.75H_2O$: C, 76.70; H, 5.19; N, 14.91. Found: C, 76.68; H, 5.20; N, 14.94.

Ru(1a)$_2$(PF$_6$)$_2$. A solution of 0.25 g (0.81 mmol) of **1a** and 0.10 g (0.40 mmol) of $RuCl_3$-3H_2O in 25 mL of EtOH-H_2O (1 : 1) was refluxed for 24 h. After cooling to room temperature, the reaction mixture was filtered to remove any unreacted reagents. To the filtrate was added 0.13 g of NH_4PF_6 to provide 0.35 g of dark purple solid, which was chromatographed on alumina eluting with CH_3CN-toluene (1 : 1). The early orange fractions gave 25.0 mg of desired complex. ^{1}H NMR (CD_3CN, 300 MHz) δ 9.06 (s, 2H, H3 and H5), 8.97 (d, 2H, *J*=4.5 Hz, H2''' and H6'''), 8.67 (d, 2H, *J*=7.9 Hz, H3' and H3"), 8.67 (d, 2H, *J*=4.8 Hz, H2'"), 8.14 (d, 2H, *J*=4.5 Hz, H3''' and H5'''), 7.97 (dd, 2H, *J*=7.8, 1.2 Hz, H4' and H4"), 7.42 (dd, 2H, *J*=5.5, 1.5 Hz, H6' and H6"), 7.19 (dd, 2H, *J*=7.8, 4.8 Hz, H5' and H 5"). LC-MS, m/e (rel. intensity) 721 (100, RuL_2^{2+}), 310 (85, L). Anal. Calcd for $RuC_{40}H_{28}N_8P_2F_{12}$: C, 47.48; H, 2.77; N, 11.08. Found: C, 47.64; H, 2.75; N, 11.10. The latter fractions gave 0.15 g of dark purple solid which has not as yet been identified.

Ru(1b)$_2$(PF$_6$)$_2$. A solution of 0.22 g (0.60 mmol) of **1b** and 0.07 g (0.27 mmol) of $RuCl_3$-3H_2O in 25 mL of EtOH-H_2O (1 : 1) was refluxed for 24 h. After cooling to room temperature, the reaction mixture was filtered to remove any unreacted reagents. To the filtrate was added 0.18 g of NH_4PF_6 to provide 126.0 mg (37%) of orange red solid which was recrystallized from CH_3CN-toluene (1 : 1) to give 84 mg of orange red crystals. ^{1}H NMR (CD_3CN, 300 MHz) δ 8.91 (d, 2H, *J*=5.8 Hz, H2''' and H6'''), 7.64 (d, 2H, *J*=7.9 Hz, H4' and H4"), 7.55 (d, 2H, *J*=5.8 Hz, H3''' and H5'''), 7.33 (dd, 2H, *J*=5.5, 1.2 Hz, H6' and H6"), 7.10 (dd, 2H, *J*= 7.8, 5.5 Hz, H5' and H5"), 3.29 (t, 2H, *J*=7.0 Hz), 3.17 (t, 2H, *J*=7.0 Hz). LC-MS, m/e (rel. intensity) 825 (87, RuL_2^{2+}), 362 (85, L). Anal. Calcd for $RuC_{48}H_{36}N_8P_2F_{12}$: C, 51.66; H, 3.23; N, 10.04. Found: C, 51.72; H, 3.21; N, 10.02.

Ru(tpy)(1b)(PF$_6$)$_2$. A mixture of 0.14 mg (0.32 mmol) of Ru(tpy)Cl_3 and 0.13 g (0.35 mmol) of **1b** in 20 mL of EtOH-H_2O (1 : 1) was refluxed for 24 h. After cooling to room temperature, the reaction mixture was filtered. To the filtrate was added 105 mg (0.64 mmol) of NH_4PF_6 to give 0.30 g (93%) of orange red precipitate, which was chromatographed in alumina eluting with CH_3CN: toluene (1 : 1). The early fractions afforded orange red crystals. ^{1}H NMR (CD_3CN, 300 MHz) δ 8.91 (d, 2H, *J*=3.8 Hz, H2''' of **1b**), 8.73 (d, 2H, *J*=8.2 Hz, H3' and H3" of tpy), 8.50 (d, 2H, *J*=8.0 Hz, H3 and H5 of tpy), 8.39 (t, 1H, *J*=8.2 Hz, H4 of tpy), 7.95 (td, 2H, *J*=7.8, 1.2 Hz, H4' and H4" of tpy), 7.62 (d, 2H, *J*=7.8 Hz, H4' and H4" of **1b**), 7.56 (d, 4H, *J*= 5.5 Hz, H3''' of **1b** and H6' and H6" of tpy), 7.28 (dd, 2H, *J*=8.0, 4.8 Hz, H5' and H5" of tpy), 7.10 (d, 2H, *J*=5.5 Hz, H6' and H6" of **1b**), 7.02 (dd, 2H, *J*=7.8, 5.5 Hz, H5' and H5" of **1b**), 3.30 (t, 2H, *J*=7.7 Hz), 3.18 (t, 2H, *J*=7.7 Hz). LC-MS, m/e (rel. intensity) 696 (45, RuL_2^{2+}), 362 (85, **1b**), 233 (100, **1a**). Anal. Calcd for $RuC_{39}H_{29}N_7P_2F_{12}$: C, 47.46; H, 2.94; N, 9.94. Found: C, 47.56; H, 2.92; N, 9.92.

Ru(tpy)(1b$^+$-CH$_3$)(PF$_6$)$_2$I. A solution of 40.0 mg (0.04 mmol) of Ru(tpy)(**1b**)$(PF_6)_2$ and 0.5 mL of CH_3I in 10 mL of acetone was stirred for 12 h. A dark red precipitate was collected to give 30.0 mg of desired product and concentration of the filtrate gave additional 13 mg of dark red solid (overall yield 94%). ^{1}H NMR (CD_3CN, 300 MHz) δ 8.94 (d, 2H, *J*=6.4 Hz, H2''' of **2**), 8.75 (d, 2H, *J*=8.3 Hz, H3' and H3" of tpy), 8.51 (d, 2H, *J*=8.0 Hz, H3 and H5 of tpy), 8.41 (t, 1H, *J*=8.2 Hz, H4 of tpy), 8.34 (td, 2H, *J*=7.8, 1.2 Hz, H4' and H4" of tpy), 8.30 (d, 2H, *J*=6.4 Hz, H3''' of **1b**), 7.95 (t, 2H, *J*=7.7 Hz, H4' and H4" of **1b**), 7.66-7.62 (m, 4H, H6' and H6" of tpy and H4' and H4" of **1b**), 7.29 (dd, 2H, *J*=8.0, 4.8 Hz, H5' and H5" of tpy), 7.13 (d, 2H, *J*= 5.6 Hz, H6' and H6" of **1b**), 7.04 (dd, 2H, *J*=7.6, 5.9 Hz, H 5' and H5" of **1b**), 4.49 (s, CH_3), 3.34 (t, 2H, *J*=7.7 Hz), 3.20 (t, 2H, *J*=7.7 Hz). Anal. Calcd for $RuC_{40}H_{32}N_7P_2F_{12}I$: C, 42.55; H, 2.84; N, 8.69. Found: C, 42.48; H, 2.85; N, 8.73.

Ru(1b$^+$-CH$_3$)$_2$(PF$_6$)$_2$I$_2$. To a solution of 30.0 mg (0.027 mmol) of Ru(**1b**)$_2(PF_6)_2$ in 20 mL of acetone was added 1.5 mL of CH_3I. The resulting mixture was refluxed for 12 h to afford 22.0 mg of red precipitate. Concentration of the solvent gave an additional 10 mg of desired product (overall yield 85%). ^{1}H NMR (CD_3CN, 300 MHz) δ 8.95 (d, 2H, *J*=6.4 Hz, H2'"), 8.38 (d, 2H, *J*=6.4 Hz, H'"), 7.66 (d, 2H, *J*=7.9 Hz, H4' and H4"), 7.51 (dd, 2H, *J*=5.5, 1.2 Hz, H6' and H6"), 7.15 (dd, 2H, *J*=7.8, 5.5 Hz, H5' and H 5"), 4.49 (s, CH_3), 3.35 (t, 2H, *J*=7.5 Hz), 3.21 (t, 2H, *J*=7.5 Hz). Anal. Calcd for $RuC_{50}H_{42}N_8P_2F_{12}I_2$: C, 42.89; H, 3.00; N, 8.01. Found: C, 43.02; H, 2.98; N, 8.03.

Results and Discussion

Synthesis

The ligands were prepared by either employing previously reported method or modification of such a method.[9] The morpholino enamines **2** were reacted with 4-pyridinecarboxaldehyde (**3**), followed by treatment with NH_4OAc to afford the terpyridines **1** which incorporated an additional 4-pyridyl ring at the 4'-position of 2,2';6',2"-terpyridine and 3,3';5',3"-bisdimethylene bridged derivative.

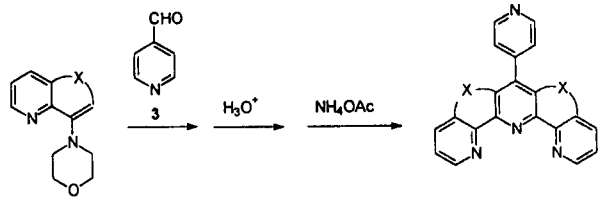

The morpholine enamine of 2-acetylpyridine (**2a**) is a relatively labile species and substantially lost during its distillation under reduced pressure. Reaction of **2a** with 4-pyridinecarboxaldehyde (**2**) resulted in a 20% yield of 4'-(4-pyridyl)-2,2';6',2"-terpyridine (**1a**). The yield was significantly improved in the reaction of **2b** with **3** to afford **1b** in 56% yield. Our ultimate interest in such molecules is the preparation and studies of metal complexes possessing remote functionalization. To this end we tried to form a bis-complex with ruthenium. Reaction of **1a** with $RuCl_3$-3H_2O provided bis-complex in only 3% yield while the bis-dimethylene annelated analog **1b** formed a similar complex in 37% yield. The dimethylene bridges in **1b** hold the ter-

Table 1. Selected ^{1}H NMR spectral data for the aromatic protons of **1** and its Ru(II) complexes

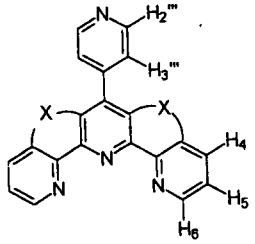

		Chemical shifts (ppm)							
X	Compound	H3'	H4'	H3	H4	H5	H6	H2'''	H3'''
H, H	**1a**[a]	8.79-8.61	-	8.79-8.61	7.88	7.35	8.79	−8.61	7.78
H, H	$Ru(\mathbf{1a})_2(PF_6)_2$	9.06	-	8.97	7.97	7.43	7.43	8.67	8.14
$-(CH_2)_2-$	**1b**	-	-	-	7.58	7.29	8.75	8.79	7.19
$-(CH_2)_2-$	$Ru(\mathbf{1b})_2(PF_6)_2$	-	-	-	7.64	7.10	7.33	8.91	7.55
$-(CH_2)_2-$	$Ru(\mathbf{1b}^+\text{-Me})_2(PF_6)_2I_2$	-	-	-	7.66	7.15	7.51	8.95	8.38
$-(CH_2)_2-$	$Ru(tpy)(\mathbf{1b})(PF_6)_2$	-	-	-	7.62	7.02	7.10	8.91	7.56[b]
		8.74	8.39	8.50	7.95	7.27	7.56[c]	-	-
$-(CH_2)_2-$	$Ru(tpy)(\mathbf{1b}^+\text{-Me})(PF_6)_2I$	-	-	-	7.64	7.04	7.13	8.94	8.30[b]
		8.75	8.34	8.1	7.95	7.29	7.64[c]	-	-

[a] Data obtained from 80 MHz ^{1}H NMR spectrum. [b] Chemical shifts of **1b** moiety. [c] Chemical shifts of 2,2';6',2"-terpyridine moiety.

dentate chelating moiety in a cavity shaped conformation which is favorable for the desired complexation. Relatively low yields are presumably due to cyclometallation pathways which might compete through other conformation of **1a** as well as complexation of the extra pyridyl moiety of **1a** and **1b**.

Reaction of $Ru(tpy)Cl_3$ with **1b**, however, gave a mixed complex $Ru(tpy)(\mathbf{1b})^{2+}$ in 94% yield. These ruthenium complexes were readily methylated by the reaction with CH_3I to afford corresponding N-methylpyridinium salts in over 85% yield while direct methylation of **1b** with CH_3I resulted in mixtures of salts.

$$Ru(tpy)Cl_3 \xrightarrow{\mathbf{1b}} Ru(tpy)(\mathbf{1b})(PF_6)_2 \xrightarrow{CH_3I} Ru(tpy)(\mathbf{1b}^+\text{-Me})(PF_6)_2I$$

Properties

NMR Spectra. The NMR spectral data of the ligand **1** and their Ru(II) complexes are summarized in Table 1. Coordination resulted in a significant downfield shift for the proton resonances except H5(H5") and H6(H6"). These two protons were upfield-shifted by 0.16-0.19 and 1.42 ppm for H5(H5") and H6(H6"), respectively. The H6(H6") protons are directed somewhat toward the shielding region of the central pyridine ring of the neighboring ligand, resulting in considerable shielding of these protons. The shielding of the more remote H5(H5") may be explained in a similar fashion. At the same time, the shielding effects on H5(H5") and H6(H6") are somewhat compensated by deshielding effects due to the electron-withdrawing 4-pyridyl ring at 4'-position of the orthogonal ligand. Thus these two protons were shifted downfield by 0.16 and 0.22 ppm, respectively, compared to the corresponding resonances of $Ru(tpy)_2^{2+}$.[10] Similar changes were observed when comparing the chemical shifts of H5 and H6 of the 2,2';6',2"-terpyridine moiety in $Ru(tpy)(\mathbf{1b})^{2+}$ to the corresponding protons of $Ru(tpy)_2^{2+}$. Methylation of $Ru(\mathbf{1b})_2^{2+}$ and $Ru(tpy)(\mathbf{1b})^{2+}$ resulted in considerable deshielding of all protons by 0.05-0.83 ppm.

Table 2. Electronic absorption data for Ru(II) complexes

Complexes	λ_{max} (ε) (1.0×10^{-5} M in CH_3CN)
$Ru(\mathbf{1b})_2(PF_6)_2$	230 (45,450), 300 (40,000), 310 (45,640)
	338 (31,180), 358 (38,000), 480 (17,090)
$Ru(\mathbf{1b}^+\text{-Me})_2(PF_2)_2I_2$	
	243 (68,550), 298 (39,550), 310 (39,180)
$Ru(tpy)(\mathbf{1b})(PF_2)_2$	343 (29,270), 358 (37,090), 484 (17,270)
	268 (39,550), 308 (69,550), 358 (28,000)
$Ru(tpy)(\mathbf{1b}^+\text{-Me})$	478 (20,730)
$(PF_6)_2I$	230 (45,000), 270 (38,640), 308 (57,450)
	360 (25,450), 480 (19,090)

Two benzylic methylene protons in **1b** were not equivalent and being mobile on the NMR time scale, exhibited two triplets at 2.91 and 2.67 ppm, which are somewhat ($\Delta\delta$ 0.1 and 0.34, respectively) upfield-shifted compared to the literature value[9] (δ 3.01, eight proton singlet) of corresponding protons in 3,3',5',3"-bis(dimethylene)-2,2';6',2"-terpyridine. These two resonances were shifted to 3.35 and 3.21 ppm upon complexation with ruthenium indicating the dimethylene units remain mobile.

Integrations of the ^{1}H NMR specra of $[Ru(tpy)(\mathbf{1b}^+\text{-}CH_3)]^{2+}$ and $[Ru(\mathbf{1b}^+\text{-}CH_3)_2]^{2+}$ indicate that there are 1 and 2 methyl protons (singlet δ 4.49, 3H and 6H, respectively). The chemical shifts of methyl protons were matched with the reported values[11] of the related compounds.

Electronic Spectra. Table 2 summarizes the electronic absorption data for the Ru(II) complexes and their methylated derivatives under discussion. The spectra consisted of two well defined regions (Figure 1). A relatively intense absorption generally consisting of three distinct bands was observed at shorter wavelength, 240-400 nm. This observation was readily assigned to a ligand-centered π-π* transition by comparing with the spectra of protonated 2,2';6'2"-terpyridine[12] and $Ru(tpy)_2^{2+}$.[13] As the ligand varied

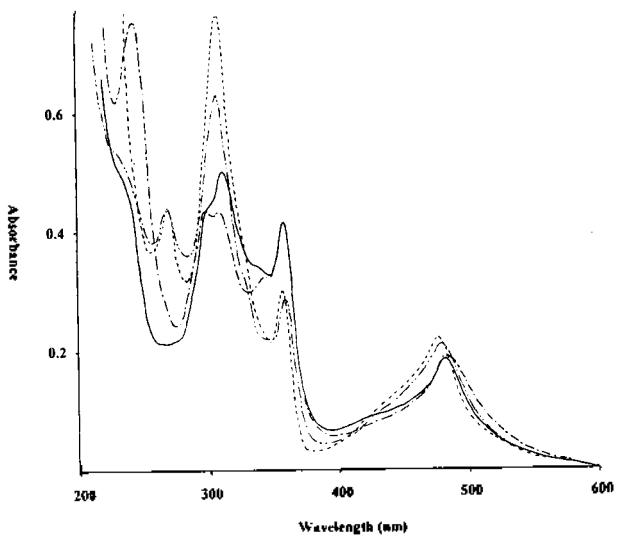

Figure 1. Electronic absorption spectra of $Ru(\mathbf{1b})_2(PF_6)_2$ (—), $Ru(tpy)(\mathbf{1b})(PF_6)_2$ (---), $Ru(tpy)(\mathbf{1b}^+\text{-}CH_3)(PF_6)_2I$ (—·—·—), and $Ru(\mathbf{1b}^+\text{-}CH_3)_2(PF_6)_2I_2$ (—··—··—) (1.0×10^{-5} M in CH_3CN).

Table 3. Redox potentials for Ru(II) complexes in CH_3CN (0.1 M TBAP) at 25 °C

Complexes	$E_{1/2}$ V (*vs.* SCE)		
	Oxidation	Reduction	
$Ru(\mathbf{1b})_2(PF_6)_2$	1.31(60)[a]	−1.25(60)	−1.52(100)
$Ru(tpy)(\mathbf{1b})(PF_2)_2$	1.38(60) 0.70(70)[b]	−0.90(60)	−1.20(90)
	0.30(70)[b]	−1.58(240)[c]	
$Ru(tpy)(\mathbf{1b}^+\text{-Me})(PF_6)_2I$	1.34(60)	−1.21(60)	−1.48(70)
$Ru(tpy)_2(PF_6)_2$	1.27(60)	−1.27(60)	−1.51(67)

[a] The values in parentheses are $\Delta E=|E_{p,a}-E_{p,c}|$. [b] Oxidation potentials are originated from the process $I^- \rightarrow I^{\cdot} + e^-$, $I + e^- \rightarrow I_2^{\cdot-}$, $I_2^{\cdot-} \rightarrow I_2 + e^-$ (cf) Oxidation potentials ($E_{1/2}$) of N-methylpyridinium iodide are 0.77(80) and 0.18(90) V. [c] Potential of the anodic peak.

from 2,2';6',2"-terpyridine to **1b**, the intensity of the absorption band at 308 nm is found to decrease showing more fine structure. This fine structure might be explained by the restriction of the mobility and increased planarity of the terpyridyl moiety in $Ru(\mathbf{1b})_2(PF_6)_2$ and $Ru(\mathbf{1b}^+\text{-Me})_2(PF_6)_2I_2$ leading to better Frank-Condon overlap between the ground and excited states. A less intense, longer wavelength band centered at 480 nm was assigned to the metal to ligand charge transfer state in which an electron is promoted from the metal t_{2g} orbital to a π^* antibonding orbital of the ligand.

Somewhat surprisingly, a distinct absorption band, arising from a MLCT state between Ru(II) and the remote N-methylpyridnium group, was not observed. The MLCT might be heavily centered on the terpyridyl moiety such that the nonplanar additional 4-pyridyl ring at the 4'-position will not significantly affect the properties of the MLCT.

Cyclic Voltammetry. The redox potentials for the Ru (II) complexes were determined by cyclic voltammetry in

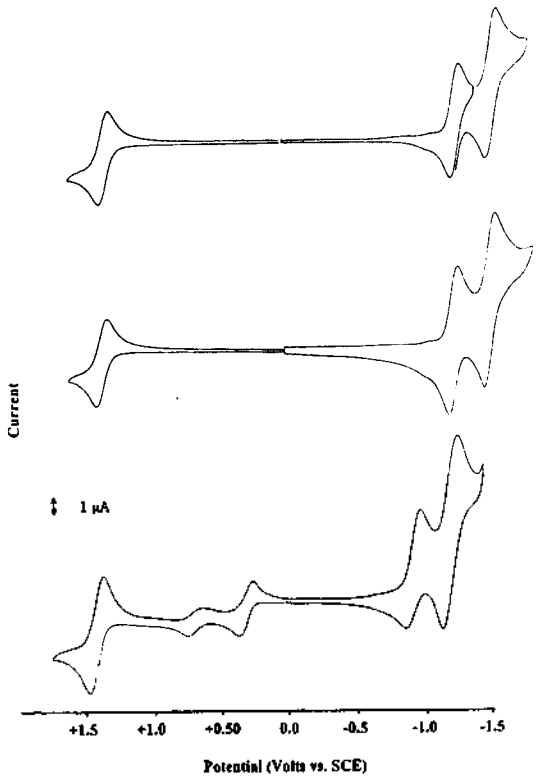

Figure 2. Cyclic voltammograms of $Ru(\mathbf{1b})_2(PF_6)_2$ (top), $Ru(tpy)(\mathbf{1b})(PF_6)_2$ (middle), and $Ru(tpy)(\mathbf{1b}^+\text{-}CH_3)(PF_6)_2I$ (bottom) in CH_3CN 0.1 M TBAP). Conditions: Pt electrode; scan rate 200 mV s^{-1}.

CH_3CN and are summarized in Table 3. All complexes showed a single one-electron reversible wave for the Ru(II)/Ru(III) oxidation in the region of 1.31-1.38 V which was shifted to more positive potential than what was observed for $Ru(tpy)_2^{2+}$ (1.27 V) (Figure 2). There were two reduction waves in the region of (-)1.20-(-)1.25 V and (-)1.48-(-)1.58 V which corresponded to the Ru(II)/Ru(I) and Ru(I)/Ru(0) couples, respectively. The first reduction was shifted to more positive potential compared to $Ru(tpy)_2^{2+}$ [(-)1.27 V)]. These observations are consistent with earlier reports that electron-withdrawing groups make Ru(II) complexes both easier to reduce and harder to oxidize.[14] For the compound $Ru(tpy)(\mathbf{1b}^+\text{-Me})(PF_2)_2I$, the first reduction at −0.90 V originated from a one electron addition to the LUMO of the N-methylpyridinium moiety compared to the reduction potentials of N-methylpyridnium salt as well as Ru(II) complex of N-methyl-4,4'-bipyridinium iodide.[15] Unfortunately, $Ru(\mathbf{1b}^+\text{-Me})_2PF_6)_2I_2$ was too insoluble to obtain a cyclovoltammogram.

In conclusion, we report the preparation 2,2';6',2"-terpyridine with extra pyridyl ring at 4'-position and its 3,3';5',3"-bis-dimethylene derivative and their Ru(II) complexes. The electronic and redox properties of the $Ru(\mathbf{1b})_2^{2+}$ complexes as well as a mixed complex $Ru(tpy)(\mathbf{1b})^{2+}$ were studied. These ruthenium complexes were methylated to form N-methylpyridinium salts which expected to affect MLCT but fail to affect the properties of MLCT presumably due to nonplanarity between the terdentate moiety and extra pyridyl ring.

References

1. (a) Juris, A.; Balzani, V.; Bargelletti, F.; Campagna, S.; Belser, P.; von Zelewsky, A. *Coord. Chem. Review* **1988**, *84*, 279. (b) Meyer, T. J. *Pure Appl. Chem.* **1986**, *58*, 1193.
2. Ghosh, K. B. *Coord. Chem. Review* **1989**, *95*, 239.
3. (a) Bock, C. R.; Conner, J. A.; Gutierrez, A. R.; Meyer, T. J.; Whitten, D. G.; Sullivan, B. P.; Nagle, J. K. *J. Am. Chem. Soc.* **1979**, *101*, 4815. (b) Meyer, T. J. *Acc. Chem. Res.* **1978**, *11*, 94.
4. (a) Haq, I.; Lincoln, P.; Suh, D.; Norden, B.; Chowdhry, B. Z.; Chaires, J. B. *J. Am. Chem. Soc.* **1995**, *117*, 4788. (b) Pyle, A. M.; Barton, J. K. *Progress Inorg. Chem.: Bioinorg. Chem.* **1990**, *38*, 413 and references therein.
5. (a) Constable, E. C. *Tetrahedron* **1992**, *46*, 10013. (b) Morgan, R. J.; Baker, A. D. *J. Org. Chem.* **1990**, *55*, 1986.
6. Bard, A. J.; Faulkner, L. R. *Electrochemical Methods, Fundamentals and Applications*; Wiley: New York, 1980, p 228.
7. Sullivan, B. P.; Calvert, J. M.; Meyer, T. J. *Inorg. Chem.* **1980**, *19*, 1404.
8. Jahng, Y.; Kim, J.-I., Na, Y. H. *Bull. Kor. Chem. Soc.* **1992**, *13*, 211.
9. Thummel, R. P.; Jahng, Y. *J. Org. Chem.* **1985**, *50*, 2407.
10. Thummel, R. P.; Jahng, Y. *Inorg. Chem.* **1986**, *25*, 2527 and references therein.
11. Bierig, K.; Morgan, R. J.; Tysoe, S.; Gafney, H. D.; Strekas, T. C.; Baker, A. D. *Inorg. Chem.* **1991**, *30*, 4898 and references therein.
12. Nakamoto, K. *J. Phys. Chem.* **1960**, *64*, 1420.
13. Constable, E. C. *Adv. Inorg. Chem. Radiochem.* **1986**, *30*, 69.
14. Elliott, C. M.; Hershenhart, E. J. *J. Am. Chem. Soc.* **1982**, *104*, 7519.
15. Sullivan, B. P.; Abruna, H.; Finklea, H. O.; Salmon, D. J.; Nagle, J. K.; Meyer, T. J. *Chem. Phys. Lett.* **1978**, *58*, 389.

Transition-State Variation in the Solvolysis of Cyclopentyl *para*-Substituted Benzenesulfonates

In Sun Koo, Kiyull Yang, Keumduck Kang, Jong Keun Park, Hyuck Keun Oh*, and Ikchoon Lee**

Department of Chemical Education, Gyeongsang National University, Chinju 660-701, Korea
**Department of Chemistry, Chonbuk National University, Chunju 560-756, Korea*
***Department of Chemistry, Inha University, Inchon 402-751, Korea*

Received October 22, 1996

Rate constants for solvolyses of cyclopentyl *para*-substituted benzenesulfonates are reported for aqueous binary mixtures with acetone, ethanol and methanol. These data are interpreted using the equations of original and extended Grunwald-Winstein relationship, Hammett equation, potential energy surface model, and quantum mechanical model. The Grunwald-Winstein plots of first-order rate constants for cyclopentyl benzenesulfonates with Y_{OTs} (based on 2-adamantyl tosylate) show a dispersion phenomenon while the extended Grunwald-Winstein plots show a good correlation (r>0.997) for the solvolyses of cyclopentyl tosylate, benzensulfonate, and *para*-chlorobenzenesulfonate. This study has shown that (i) the magnitudes of m, l and m/l associated with a change of solvent composition indicate a relatively advanced bond-breaking in the transition state for the solvolysis of cyclopentyl tosylate, (ii) the decrease of ρ_L value with solvent change from pure ethanol to pure water implies a product-like transition state, where bond breaking is much more progressed than bond formation (iii) both the potential energy surface and quantum mechanical models are applicable for the prediction of the transition state variation involving more product-like S_N2 transition state, and (iv) the S_N2 reaction via product-like transition state appears to cause the dispersions in the original Grunwald-Winstein correlations.

Introduction

Dispersion into separate lines in the correlation of the specific rates of solvoysis of a substrate in various binary mixtures was documented[1-3] in early treatments using the Grunwald-Winstein Eq. (1).

$$\log(k/k_o)=mY+c \quad (1)$$

In Eq. (1), k and k_o are specific rates of solvolysis of a substrate in a given solvent, of solvent ionizing power Y, and in 80% ethanol, respectively, m is the sensitivity to changes in Y values, and c is a residual (constant) term. Eq. (1) is commonly written without the intercept (c), which is

not required for typical interpretations, but it is often considered as a "hidden" adjustable parameter in the correlations.[4]

In general, dispersion effects in unimolecular solvolyses[5,6] make smaller contribution to the overall linear free energy relationship (LFER) than solvent nucleophilicity effects in bimolecular solvolyses. It was suggested[2] that a second term which is governed by the sensitivity l to solvent nucleophilicity N, should be added to Eq. (1) for bimolecular solvolyses. The resulting Eq. (2) is often referred to as an extended Grunwald-Winstein equation.

$$\log(k/k_o)=mY+lN \tag{2}$$

It was also suggested that a Y scale based on 2-adamantyl tosylate solvolysis[7-9] (Y_{OTs}) should be the most appropriate, and N_{OTs} values can be obtained from Eq. (3).

$$N_{OTs}=\log(k/k_o)_{MeOTs}-0.3Y_{OTs} \tag{3}$$

The main cause of dispersion in the Grunwald-Winstein plots using Eq. (1) is the different leaving group in the solvoysis of a given substrate from that of the standard substrate used to establish the Y scale being used in the correlation.[10] Other causes of dispersion phenomenon are the resonance stabilization within benzylic carbocations and appreciable crowding in the vicinity of the reaction center.[11]

The potential energy surface (PES) model[12] for predicting transition state variation is based on the application of the Hammond postulate[13] and the Thornton's rule[14] to the reaction of a nucleophile (N) attacking a substrate (RL),

$$N(B) + RL(A) \rightarrow [N\cdots R\cdots L]^* \rightarrow N^+\text{-}R + L^- \tag{4}$$

While the PES model has been successful in many applications, one of the prominent failures of this model involved the inability of predicting the effect of changing the leaving group on transition-state structure of nucleophilic substitution reactions.[15]

Pross[16] *et al.*, and Lee *et al.*,[17] however, solved this difficulty by analyzing the effect of leaving groups on transition-state structure using a simplified quantum mechanical (QM) model. In the method of Pross *et al.*,[16] transition states are defined in terms of linear combinations of reactant configurations. This model has been shown to predict correctly the effects of nucleophiles and substrates as well as of leaving groups when applied to a limited family of reactions such as the S_N2 reaction of benzyl derivatives.

In this work, transition state variation in the solvolysis of some cyclopentyl *para*-substituted benzenesulfonates in EtOH-H_2O, MeOH-H_2O and Acetone-H_2O mixtures is investigated by applying the extended Grunwald-Winstein equation, the Hammett equation, the potential energy surface model and the quantum mechanical model.

Results and Discussion

Solvent Effects. Rate constants for solvolyses of cyclopentyl tosylate, cyclopentyl benzenesulfonate, cyclopentyl *para*-chlorobenzenesulfonate, and cyclopentyl *para*-nitrobenzenesulfonate in aqueous binary mixtures of acetone, ethanol, and methanol are reported in Table 1. In order to eliminate the dispersion phenomenon due to variation of leaving group in Grunwald-Winstein plots, we tried to correlate log k with Y_{OTs} using k values obtained in this work. The Grunwald-Winstein plots of first-order rate constants for cyclopentyl tosylate with Y_{OTs} (based on 2-adamantyl tosylate) still showed dispersions for cyclopentyl tosylate, cyclopentyl benzenesulfonate, and cyclopentyl *para*-chlorobenzenesulfonate (Figures 1, 2, and 3). However, the plot of first-order rate constants for cyclopentyl para-nitrobenzenesulfonate with Y_{OTs} (based on 2-adamantyl tosylate) showed a little dispersions (Figure 4).

Since cyclopentyl para-substituted benzenesulfonates are neither conjugated systems nor aromatic rings adjacent to the reaction center in the substrate, it can not be explained by phenomenon of the dispersion caused by differential solvation effect on the stabilized reaction center by conjugation with adjacent conjugated system or aromatic rings. Therefore such phenomenon can be explained as dispersion effect caused by other specific solvent effect or a change of reaction mechanisms according to the variation of solvent composition. In order to examine the cause of this dispersion phenomenon, we correlated using extended Grunwald-Winstein equation with the rate data in Table 1. The extended Grunwald-Winstein plots showed good correlations for cyclopentyl benzenesulfonates solvolysis (Figures.

Table 1. Rate constants(k) solvolyses of cyclopentyltosylates in aqueous binary mixtures at 25 °C

	$k\times10^4$ sec^{-1}											
v/v%	MeOH				EtOH				Acetone			
	p-CH_3	H	*p*-Cl	*p*-NO_2	p-CH_3	H	*p*-Cl	*p*-NO_2	p-CH_3	H	*p*-Cl	*p*-NO_2
100	0.115	0.171	0.407	2.59	0.0325	0.0732	0.128	0.820				
90	0.242	0.388	0.993	4.09	0.103	0.181	0.560	3.68				
80	0.515	0.908	2.26	15.8	0.254	0.430	1.34	10.4	0.0288	0.066	0.202	1.93
70	1.05	1.86	4.62	29.6	0.496	0.865	2.64	20.6	0.112	0.207	0.670	5.72
60	2.20	3.72	9.20	57.6	0.907	1.55	5.04	39.2	0.321	0.526	1.84	15.4
50	4.56	7.51	18.7	108	1.93	3.05	9.52	72.0	0.919	2.06	4.82	37.7
40	9.17	16.0	36.2	207	4.35	7.53	20.0	147	2.48	4.91	12.6	91.7
30	19.3	33.1	70.0	378	12.0	22.8	48.6	310	7.69	18.2	33.0	211
20	36.8	65.6	126	635	32.7	47.9	115	635	21.9	35.8	74.8	442
10	69.1	110	186	944	63.9	112	189	1010	59.3	84.7	148	836
0	101	177	282	1380	101	177	282	1380	101	177	282	1380

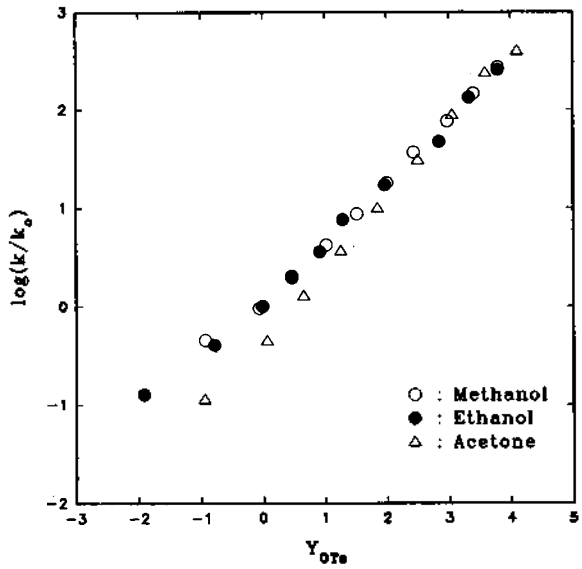

Figure 1. Logarithms of first-order rate constants for solvolyses of cyclopentyl tosylate at 25°C *vs.* Y_{OTs}.

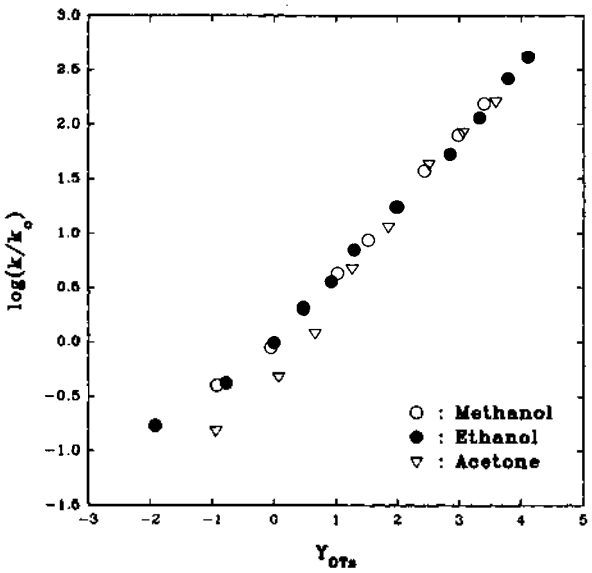

Figure 2. Logarithms of first-order rate constants for solvolyses of cyclopentyl benzenesulfonate at 25 °C *vs.* Y_{OTs}.

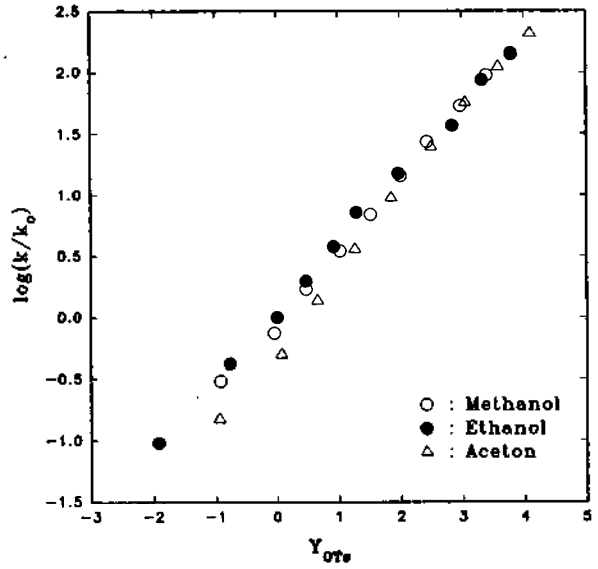

Figure 3. Logarithms of first-order rate constnats for solvolyses of cyclopentyl *para*-chlorobenzenesulfonate at 25 °C *vs.* Y_{OTs}.

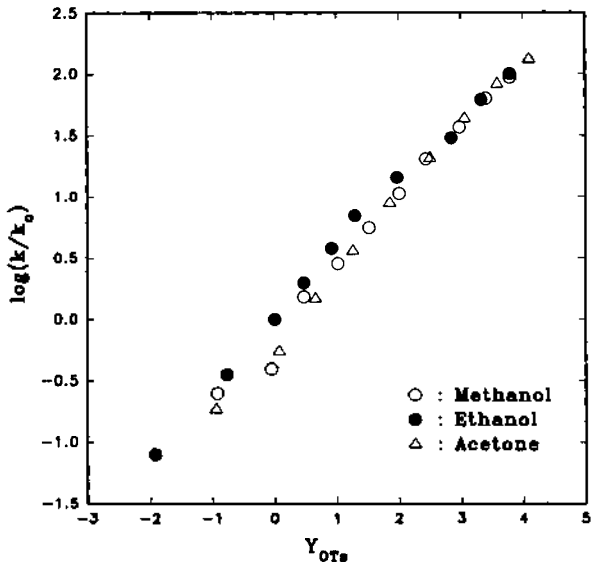

Figure 4. Logarithms of first-order rate constants for solvolyses of cyclopentyl *para*-nitrobenzenesulfonate at 25 °C *vs.* Y_{OTs}.

5, 6, 7, and 8).

The nucleophilicity parameter (*N*) has previously been shown to give considerable improvement when an *lN* term is added to the original Grunwald-Winstein correlations of the solvolyses reactions. The *m* value is changed slightly after removal of dispersion, but the associated standard errors are substantially reduced. The correlation coefficient of 0.989 in the absence of the *lN* term was improved to 0.996 with the *lN* term for cyclopentyl tosylate solvolysis. Therefore, it shows the importance of solvent nucleophilicity compared to solvent ionizing power for the solvolysis of cyclopentyl tosylate. And also, same linear free energy relationships for the solvolysis of cyclopentyl benzenesulfonate and cyclopentyl *para*-chlorobenzenesulfonate were improved with good linear correlation coefficients. This indicates that the solvolysis of cyclopentyl derivatives proceeds by predominantly S_N2 pathway with a more product-like transition state (asymmetric TS, $[N^{\delta+}\cdots C\cdots L^{\delta-}]^*$), where bond breaking is much more progressed than bond formation (vide infra). The S_N2 reaction *via* product-like transition state appears to cause the dispersions in the present Grunwald-Winstein correlations.

Substituent Effects. The Hammett plot (Figure 9) for the variation of substituents of leaving group shows a good linearity ($r \geq 0.997$) with large positive slopes, ρ_L= 0.90-1.7 in various alcohol-water solvents at 25 °C (Table 3). Relatively large ρ_L values suggest that bond breaking tends to be advanced in the transition state of the solvolysis of cyclopentyl benzenesulfonates. If we assume virtually separate ρ values for bond formation (ρ_L<0) and bond breaking (ρ_L>0),[18] positive ρ_L values obtained suggest predom-

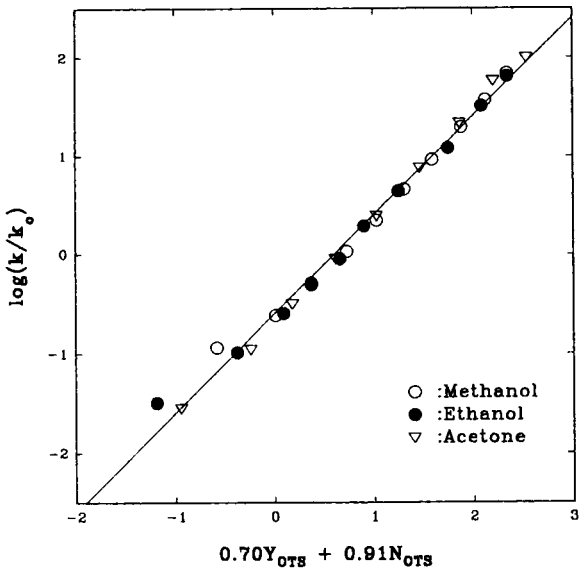

Figure 5. Plot of $\log(k/k_o)$ for cyclopentyl tosylate against $0.70Y_{OTS}+0.91N_{OTS}$ (r=0.996).

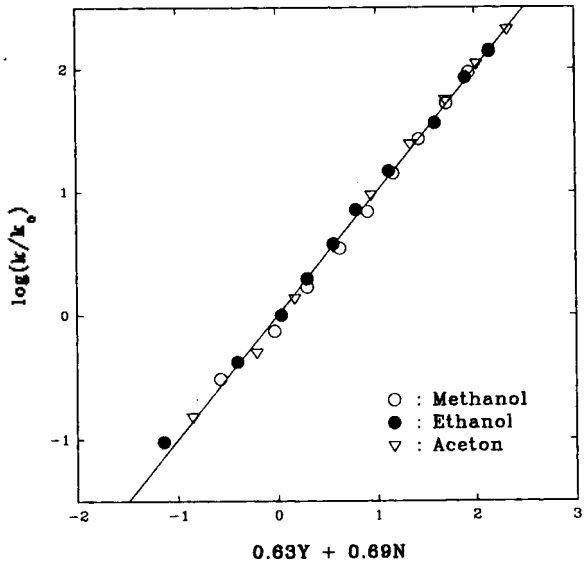

Figure 7. Plot of log (k/k_o) for cyclopentyl *para*-chlorobenzenesulfonate against $0.63Y+0.69N$ (r=0.999).

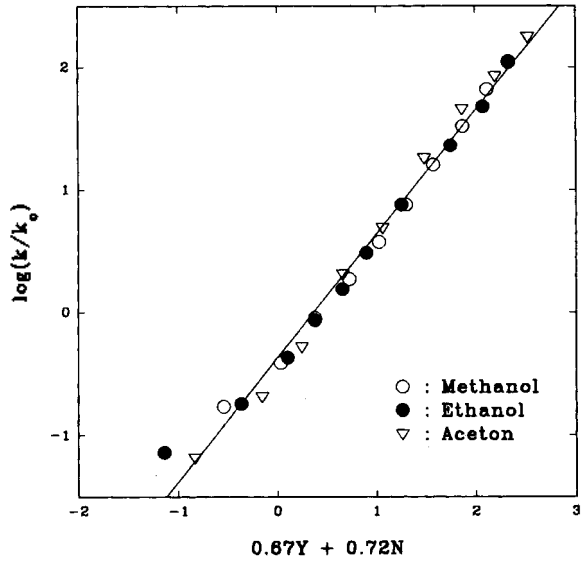

Figure 6. Plot of log (k/k_o) for cyclopentyl benzenesulfonate against $0.67Y+0.72N$ (r=0.994).

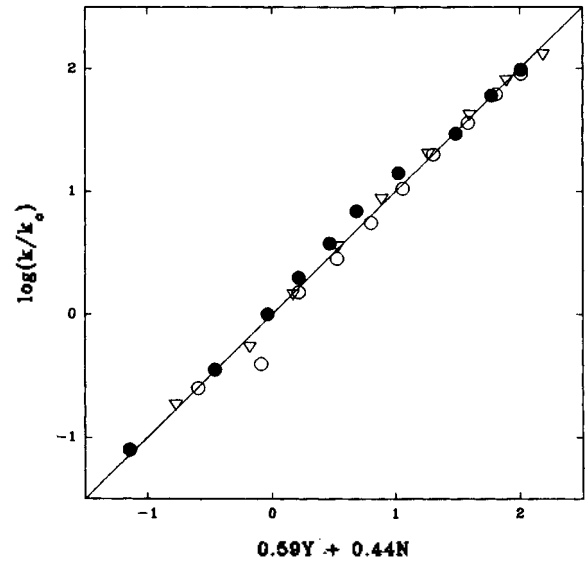

Figure 8. Plot of log (k/k_o) *for cyclopentyl para*-nitro benzenesulfonate against $0.59Y+0.44N$ (r=0.998).

inance of the bond-breaking in the transition state. The relatively loose transition state with a large degree of bond cleavage predicted for the solvolysis of cyclopentyl arenesulfonates in this work is consistent with the relatively small ρ_{XZ} values found for the S_N2 reactions of cycloalkyl derivatives.[19a] It has been shown that the magnitude of ρ_{XZ}, which is defined by Eqs. (5),[20] is inversely proportional to the tightness of the S_N2 transition state (or to the distance between reaction centers on nucleophile (X) and leaving group (Z), γ_{XZ}^*, which is the same

$$\log(k_{XZ}/k_{HA})=\rho_X\sigma_X+\rho_Z\sigma_Z+\rho_{XZ}\sigma_X\sigma_Z \quad (5a)$$

$$\rho_{XZ}=\frac{\partial\rho_Z}{\partial\sigma_X}=\frac{\partial\rho_X}{\partial\sigma_Z} \quad (5b)$$

as γ_{NL}^* Eq. (4); the larger the magnitude of ρ_{XZ}, the tighter is the transition state, *i.e.*, the shorter is the γ_{XZ}^* (or γ_{NL}^*).[21] Moreover, the ρ_{XZ} value has been found to be a relatively large constant value for the S_N2 reaction at a primary carbon ($\rho_{XZ}\cong0.3$), whereas it is a smaller constant at a secondary carbon center ($\rho_{XZ}\cong0.1$), irrespective of the size of the group attached to the reaction center. These constant ρ_{XZ} values suggest that the transition state tightness of the S_N2 reactions is tight or loose *i.e.*, γ_{XZ}^* (or γ_{NL}^*) is short or long, depending on whether the reaction center carbon is primary or secondary, but the transition state tightness varies very little with regard to the group attached to the reaction center.[19] The constancy of the transition state tightness has been confirmed by the experimental ρ_{XZ} values as well as by a high level *ab initio* MO calculations,[22] the difference in the experimental ρ_{XZ} values between the primary and secondary carbon centers of *ca.* 0.2 ($\Delta\rho_{XZ}\cong0.2$) corresponded to the

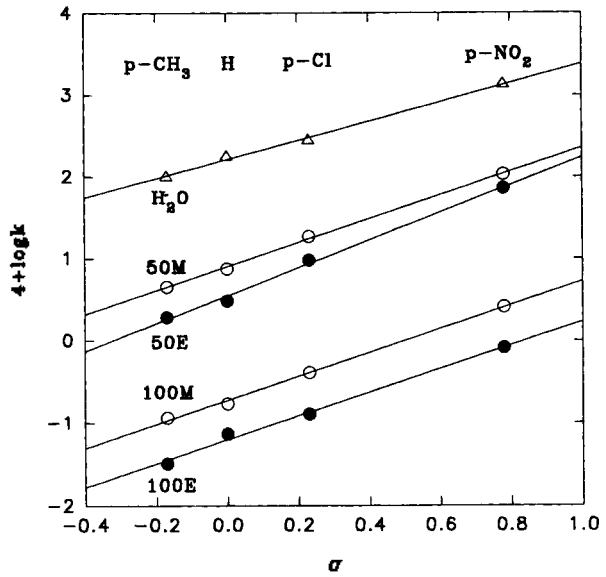

Figure 9. Hammmet plot for the solvolysis of cyclopentyl benzenesulfonates in alcohol-water at 25 °C.

Table 2. Correlation of the specific rates of solvolysis of cyclopentyl benzenesulfonates at 25 °C

Substituents	*m*	*l*	*m/l*	*r*
p-CH_3	0.70	0.91	0.77	0.996
H	0.67	0.72	0.93	0.994
p-Cl	0.63	0.69	0.91	0.999
p-NO_2	0.59	0.44	1.34	0.999

Table 3. Hammett ρ_L values for the solvolysis of cylopentyl para-substituted benzenesulfonates in alcohol-water at 25 °C

Sovlents	100E	100M	50E	50M	H_2O
ρ_L	1.74	1.54	1.55	1.26	0.92
r	0.998	1.00	0.998	0.998	0.997

$\Delta\gamma_{XZ}^*$ values of *ca.* 0.1 Å ($\Delta\gamma_{XZ}^* \cong 0.1$ Å).[19]

Since cyclopentyl derivatives used in this work have a secondary carbon reaction center and react by the S_N2 mechanism,[19a] the transition state is expected to have a rather loose structure, as evidence by the large component of S_N2 character (large *l* values) as well as by the large ρ_L values ($\rho_L \cong 1.0$-1.7). The decrease of ρ_L from pure ethanol to water (1.7→0.90) implies an increasing importance of bond making in the transition state. The transition state is therefore more product-like (more asymmetric transition state, $[N^{\delta+}\cdots C\cdots L^{\delta-}]^*$), where bond breaking is much more progressed than bond formation in ethanol than water. This is again in line with a relatively constant transition state tightness, *i.e.*, $\gamma_{NL}^* \cong$ *constant*, since a stronger nucleophile (EtOH) should lead to a shorter γ_{NC}^* with a larger γ_{CL}^* (larger γ_L), whereas a weaker nucleopile (H_2O) leads to a longer γ_{NC}^* with a shorter γ_{CL}^*, with approximately constant total tightness, *i.e.*, $\gamma_{NL}^* = \gamma_{CL}^* + \gamma_{CL}^* \cong$ constant.

Application of the PES model. The most recent and convenient method of application of the PES model is to use a More O'Ferrall type of energy surface[12] (Figure 10) in predicting the changes in the structure of the transition

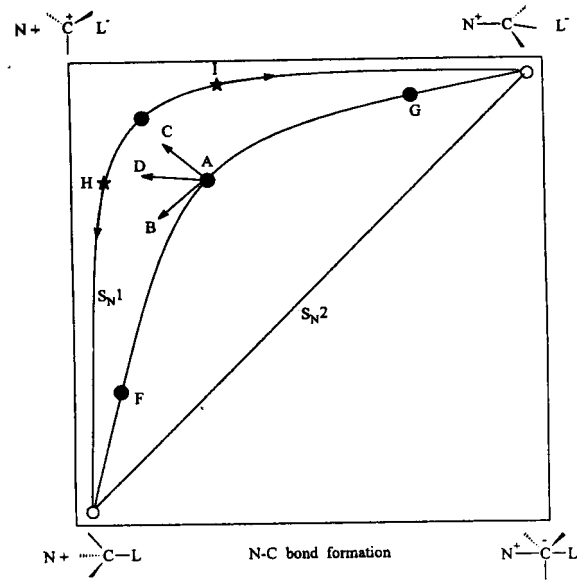

Figure 10. Potential energy surface for nucleophilic substitution of cyclopentyl benzenesulfonates; N is the nucleophile, and energy minima and maxima are repreented by circles and star marks, respectively.

state as a sustituent in the substrate, the nucleophile, or the leaving group is changed. Since it is well established that bond-breaking is more ahead of bond-making in the transition state of nucleophilic cyclopentyl sulfonates substitution, the transition state will lie on the reaction coordinate between S_N1 and S_N2 paths. It can be readily shown that both an early, F, and a late, G, transition states would not be consistent with the experimental results. Similarly simple considerations of the effects of substituents in the substrate lead us to reject the S_N1 mechanism as untenable; an electron-withdrawing substituent in the leaving group should stabilize the upper left corner which is on the reaction coordinate of the S_N1 path and the first transition state H will move toward reactants corner (the second transition state, I, away from products corner) hence C-L bond cleavage should decrease in contrary to the experimental results; the small ρ_L values obtained for a higher ionizing power solvent suggest a shorter C-L bond in the transition state. The increase in ionizing power of solvent mixture should enhance the leaving ability by assisting the leaving group L to depart more easily causing a slight increase in the length of the C-L bond. On the PES diagram, the increase in the ionizing power stabilizes the upper corner, and this should cause the transition state A to move to, *e.g.* D which is obtained as a vector sum of AB and AC. Thus vector AD will be somewhere in between the vector AB and AC depending on the magnitudes of the two vectors. The PES model now predicts that the increase in the ionizing power should always lead to a longer N-C bonds irrespective of whether perpendicular or parallel effect is stronger. This is consistent with the experimental results since smaller ρ_L values clearly indicated a shorter C-L together with a longer N-C bond (keeping approximately constant γ_{NL}^*) as the ionizing power of solvents is increased in water. Thus we conclude that the PES model predicts transition state variation correctly for S_N2 reaction of cy-

Table 4. The structural effects of the key configurations on the reaction complex, [N···R···X]

Configuration	Structural effect	
	N-R	R-X
BA	loose	tight
B^+A^-	tight	loose
BA*	loose	loose

clopentyl benzenesulfonates.

Application of the QM model. In general four types of interactions are involved in the perturbation of a system, A, by another, B: electrostatic, polarization, exchange repulsion, and charge transfer interactions.[17,23] The former two are long range whereas the latter two are short range components of intersystem interactions. Pross and Shaik[16] considered only the two, polarization and charge transfer, in their quantum mechanical description of transition state structure. They expressed various states of the reaction complex as a linear combination of the three configurations; ground BA, polarized BA* and charge transferred B^+A^- configurations. In a nucleophilic substitution reaction, B may be a nucleophile N and A a substrate RX with a leaving group X. Analysis of bonding characteristics and the relative contribution to the structure of the transition state of the three key configurations allow us to predict how the transition state will change as a result of a given perturbation. Examination of the structural implications associated with each configuration using an MO and VB description led Pross and Shaik to a set of simple rules for prediction the structural effects of the three configurations on the reaction complex as presented in Table 4. Let us now apply the QM model based on these rules of structural effects. Application of the model to the predictions of effects of the nucleophile and substrate is entirely analogous to that for the benzyl and sulfonyl system.[15,24] An increase in the nucleophile strength (ethanol) will increase electron donating ability of the nucleophile and hence increase the contribution of the B^+A^- configuration to the transition state. Reference to Table 4 suggests that as a consequence both nucleophile-substrate (N-C) bond formation and substrate-leaving group (C-L) bond should increase. The experimental results obtained in this work support these predictions. It can be seen that the ρ_L value increases in the order of nucleophilicity (Table 3). Increasing electron withdrawing ability in the leaving group has the effect of increasing leaving ability, which will result in lowering the energy of the B^+A^- and BA* configuration in which electrons are already largely localized on the leaving group. Thus the contributions of these two configurations to the transition state will increase. Reference to Table 4 also suggests a looser C-L bond while the effect on N-C bond length is uncertain since two opposing effects are predicted. The experimental *m/l* values increase in the order X=p-CH_3<H<p-Cl<p-NO_2, where X is the substituent in the leaving group ring since the bond-breaking is slightly more advanced in the transition state. Therefore, quantum mechanical approach is well established to propose the product like transition state for the solvolysis of cyclopentyl benzenesulfonates.

Conclusions

This study has shown: (i) the magnitudes of *m*, *l* and *m/l* associated with a change of solvent composition indicate that bond-breaking in the transition state is relatively more advanced, (ii) the decrease in ρ_L from pure ethanol to pure water suggests that a more product-like transition state (asymmetric TS, $[N^{\delta+}\cdots C\cdots L^{\delta-}]^{\neq}$), where bond breaking is much more progressed than bond formation is obtained upon increasing solvent nucleophilicity, (iii) both the PES and QM models correctly predict the transition state variation to a more product-like S_N2 transition state, and (iv) the dispersions in the Grunwald-Winstein correlations in the present studies are caused by the product-like S_N2 transition state structure.

Experimental

Cyclopentyl para-substituted benzenesulfonates were prepared by the previous method.[25] Gr grade methanol, ethanol and acetone (Merck) were used without further purification. Water was used after purification as described in the previous report.[26] Kinetic measurements were done conductometrically using the same apparatus and thermostatic bath as before.[26] Pseudo-first order rate constants were determined by the LSKIN program.[27] Rate constants were accurate to ±3%.

Acknowledgment. This work was supported by Korea Science and Engineering Foundation.

References

1. Winstein, S.; Grunwald, E. *J. Am. Chem. Soc.* **1948**, *70*, 846.
2. Winstein, S.; Grunwald E.; Jones, H. W. *J. Am. Chem. Soc.* **1951**, *73*, 2700.
3. Fainberg, A. H.; Winstein, S. *J. Am. Chem. Soc.* **1956**, *78*, 2770.
4. Bentley, T. W.; Bowen, C. T.; Morten, D. H.; Schleyer, P. v. R. *J. Am. Chem. Soc.* **1981**, *103*, 5466.
5. Winstein, S.; Fainberg, A. H.; Grunwald, E. *J. Am. Chem. Soc.* **1957**, *79*, 4146.
6. Fainberg, A. H.; Winstein, S. *J. Am. Chem. Soc.* **1957**, *79*, 1597.
7. Bentley, T. W.; Llewellyn, G. *Prog. Phys. Org. Chem.* **1990**, *17*, 121.
8. Schadt, F. L.; Bentley, T. W.; Schleyer, P. v. R. *J. Am. Chem. Soc.* **1976**, *98*, 7667.
9. Bentley. T. W.; Schleyer, P. v. R. *J. Am. Chem. Soc.* **1976**, *98*, 7656.
10. Fainberg, A. H.; Winstein, S. *J. Am. Chem. Soc.* **1957**, *79*. (a) 1602; (b) 1608.
11. Liu, K.-T.; Sheu, H.-C. *J. Org. Chem.* **1991**, *56*, 3021.
12. More O'Ferrall, R. A. *J. Chem. Soc.(B)* **1970**, 274.
13. Hammond, G. S. *J. Am. Chem. Soc.* **1955**, *77*, 334.
14. Thornton, E. R. *J. Am. Chem. Soc.* **1967**, *89*, 2915.
15. Westaway, K. C.; Ali, S. F. *Can. J. Chem.* **1979**, *57*, 1354.
16. Pross, A.; Shaik, S. S. *J. Am. Chem. Soc.* **1981**, *103*, 3702.
17. Lee, I.; Song, C. H. *Bull. Korean Chem. Soc.* **1986**, *7*,

186.
18. Johnson, C. D. *The Hammett Equation*; Cambrige Univ. Press: Cambrige, 1973; Chap. 1.
19. (a) Oh, H. K.; Kwon, Y. B.; Cho, I. H.; Lee, I. *J. Chem. Soc. Perkin Trans. 2*, **1994**, 1697. (b) Oh, H. K.; Kwon, Y. B.; Chung, D. S.; Lee, I. *Bull. Korean Chem. Soc.* **1995**, *16*, 827. (c) Lee, I. *Chem. Soc. Rev.* **1995**, *24*, 223.
20. (a) Lee, I. *Chem. Soc. Rev.* **1990**, *19*, 317. (b) Lee, I. *Adv. Phys. Org. Chem.* **1992**, *27*, 57.
21. Lee, I. *J. Phys. Org. Chem.* **1992**, *5*, 736.
22. Lee, I.; Kim, C. K.; Chung, D. S.; L, B. S. *J. Org. Chem.* **1994**, *59*, 4490.
23. (a) Murrell, J. M.; Randic, M.; Williams, D. *J. Proc. Roy. Soc.* **1965**, *A284*, 566. (b) Fueno, T.; Nagase, S.; Tatsumi, K.; Yamaguchi, K. *Theoret. Chim. Acta* **1972**, *26*, 48. (c) Fukui, K.; Fujimoto, H. *Bull. Chem. Soc. Jpn.* **1968**, *41*, 1989. (d) Morokuma, K. *J. Chem. Phys.* **1971**, *55*, 1236. (e) Kollman, P. *Accounts Chem. Res.* **1977**, *10*, 365. (f) Lee, I. *Prog. Chem. and Chem. Industry* **1977**, *17*, 383.
24. Lee, I.; Koo, I. S. *Tetrahedron* **1983**, *39*, 1803.
25. Oh, H, K.; Kwon, Y. B.; Cho, I. H.; Lee, I. *J. Chem. Soc., Perkin Trans. 2* **1994**, 1697.
26. Koo, I. S.; Yang, K.; Kang, K.; Oh, H. K.; Lee, I. *Bull. Korean Chem. Soc.* **1996**, *17*, 520.
27. Bentley, T. W.; Carter, G. E.; Harris, H. C. *J. Chem. Soc., Perkin Trans. 2* **1985**, 938.

pH and Micellar Effects on the Quenching of Tris(2,2'-bipyridine)Ruthenium(II) Luminescence by 1-Alkyl-4,4'-bipyridinium: Evidence of Deep Embedment of the Quencher Cations in Sodium Dodecyl Sulfate Micelle

Joon Woo Park* and Yu Na Kim

Department of Chemistry, Ewha Womans University, Seoul 120-750, Korea
Received October 28, 1996

The effects of pH and sodium dodecyl sulfate (SDS) micelle on the quenching of $Ru(bpy)_3^{2+}$ luminescnce by N-alkyl-4,4'-bipyridinium ions ($RBPY^+$: R=methyl, octyl, dodecyl, benzyl) were investigated. In the absence of SDS, the quenching rate at pH 2 is similar to that of the corresponding methylalkyl viologens and much greater than that in pH 8 solution due to greater reducibility of the protonated form of $RBPY^+$ ($HRBPY^{2+}$). The quenching rate at pH 2 is strongly enhanced by the presence of SDS, while that at basic pH is greatly retarded. These observations are explained by deep embedment of $RBPY^+$ into the hydrophobic hydrocarbon region of the micelle, whereas $Ru(bpy)_3^{2+}$ and $HRBPY^{2+}$ locate in the Stern layer of the micelle.

Introduction

The electron transfer quenching of luminescence from tris (α,α'-diimine)ruthenium(II) complexes by viologens has been extensively investigated in relation to the development of light to chemical energy conversion schemes[1-9] and photosensitized reductive transformation of organic compounds[10,11] where viologens behave as electron mediators. The rate of the quenching reactions is greatly enhanced by the presence of anionic micelles such as sodium dodecyl sulfate (SDS), largely due to condensation of the electron donor and acceptor pairs in the potential field of the anionic microparticles by electrostatic interaction.[3-9] However, different degree of embedment of viologens into micellar interface depending on the alkyl chain length also influences the surface diffusion of the viologens in micelles and thus the quenching rate.[4,6,7]

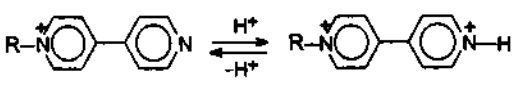

Basic Form ($RBPY^+$) Acidic Form ($HRBPY^{2+}$)

1-alkyl-4,4'-bipyridinium ions ($RBPY^+$) undergo the following acid-base equilibrium. The acidic form ($HRBPY^{2+}$) has structural similarity to viologens, while the basic form is a substituted pyridinium ion which can be considered as an analog of coenzyme NAD^+.[12] Because of these interesting characteristics, the pH-dependent electrochemical[13-16] and spectroscopic[14,15,17] behaviors of the compounds as well as the ability of the compounds as electron mediators in redox reactions in homogeneous media have been investigated.[18-20] An nmr study indicated that the bipyridine moiety of $RBPY^+$ intercalates between the hydrocarbon chains of the SDS micelle.[21] In this paper, we have studied the emission quenching of $Ru(bpy)_3^{2+}$ by various $RBPY^+$ in acidic and basic solutions. The opposite effect of SDS on the quenching reaction rate depending on pH is discussed in terms of difference of the locations of $HRBPY^{2+}$ and $RBPY^+$ in the micelle.

Experimental Section

Sodium dodecyl sulfate was obtained from Fluka and was purified by recrystallization from ethyl alcohol after washing with diethyl ether. Chloride salts of 1-alkyl-4,4'-bi-